J Mater Sci (2011) 46:1806–1813
DOI 10.1007/s10853-010-5004-4

# Phase formation and dielectric properties of $Ba_{0.5}Sr_{0.5}TiO_3$ by slow injection sol–gel technique

**R. Balachandran · H. K. Yow · B. H. Ong · K. B. Tan · K. Anuar · W. T. Teoh · M. N. Ahmad Fauzi · S. Sreekantan · V. Swaminathan**

Received: 8 May 2010 / Accepted: 12 October 2010 / Published online: 26 October 2010


**Abstract** A simple sol–gel process incorporating slow precursor injection technique was employed to synthesize homogeneous $Ba_{0.5}Sr_{0.5}TiO_3$ nano powders. The $Ba_{0.5}Sr_{0.5}TiO_3$ samples were subjected to calcination temperatures from 600 to 1,100 °C and sintering temperatures from 1,250 to 1,350 °C for the study of phase formation, crystallite size, particle distribution, and dielectric properties. Single phase $Ba_{0.5}Sr_{0.5}TiO_3$ with a cubic perovskite structure was successfully synthesized after calcination at 800 °C. The average size of the nano particles is 42 nm with a narrow size distribution, and a standard deviation of 10%. The highest values recorded within the investigated range for dielectric constant, and dielectric loss measured at 1 kHz are 1,164 and 0.063, respectively, for $Ba_{0.5}Sr_{0.5}TiO_3$ pellets calcined at 800 °C and sintered at 1,350 °C. Leakage current density measured at 5 V for the $Ba_{0.5}Sr_{0.5}TiO_3$ pellet was found to be 49.4 pA/cm$^2$.

R. Balachandran (✉) · H. K. Yow · B. H. Ong
Faculty of Engineering, Multimedia University,
63100 Cyberjaya, Selangor, Malaysia
e-mail: balachandran.ruthramurthy@mmu.edu.my

K. B. Tan
Department of Chemistry, Faculty of Science, Universiti Putra Malaysia, 43400 Serdang, Selangor, Malaysia

K. Anuar
Department of Chemistry, Universiti Putra Malaysia,
43400 Serdang, Selangor, Malaysia

W. T. Teoh
Department of Environmental Engineering, Nagaoka University of Technology, Niigata 940-2188, Japan

M. N. Ahmad Fauzi · S. Sreekantan
School of Materials & Mineral Resource Engineering,
Engineering Campus, Universiti Sains Malaysia,
14300 Nibong Tebal, Malaysia

V. Swaminathan
School of Material Science and Engineering, Nanyang Technological University, Singapore 639798, Singapore

## Introduction

Barium Strontium Titanate ($Ba_xSr_{1-x}TiO_3$) (BST) oxide system has attracted much attention for applications in electronic devices due to its high dielectric constant, high breakdown field strength, small dielectric loss, and good thermal stability. In particular, BST thin film is considered one of the most promising dielectric materials for high density capacitors in dynamic random access memories (DRAMs) [1, 2] with high charge storage density and low leakage current density which translate to minimum refreshing time required. The composition can be easily controlled due to the absence of volatile lead oxide [3]. BST thin films are expected to replace the conventional $SiO_2$ or $Ta_2O_5$ dielectrics which cannot provide the required charge storage capacity. On the other hand, $Ba_{0.5}Sr_{0.5}TiO_3$ has been found to be an attractive choice by combining the structural stability of $SrTiO_3$ and high permittivity of ferroelectric $BaTiO_3$ [4].

Various film deposition techniques such as metal-organic chemical vapor deposition (MOCVD) [5], pulsed laser deposition (PLD) [6, 7], charge liquid cluster beam (CLCB) method [8], sputtering [3, 4, 9–11], and sol–gel methods [12] have been commonly used for the synthesis of the BST films. However, the film density and thickness uniformity which ultimately influence the dielectric performance of the BST films are strongly dependent on the particle size and homogeneity of the BST powder ceramics. Hence, precise control of particle size and homogeneous

distribution of nano-scale BST particles are important prerequisites for the deposition of high quality BST films.

In order to apply BST thin films in DRAM capacitors, it is crucial to achieve extremely low leakage current and as highly possible as dielectric constants [13]. In memory devices, small leakage current (<100 nA/cm$^2$) level is necessary for stable operation in thin dielectric layers. If 1.5 V voltage is applied to BST film of 50 nm, a leakage current density level of less than 100 nA/cm$^2$ is therefore required for the resistivity of the material to be larger than $3 \times 10^{12}$ Ω cm [14]. It is understood that dielectric constant, dielectric loss, and leakage current of BST thin films depend upon the deposition method, composition, dopant, electrode, microstructure, interfacial quality, and thickness of the films [15].

In general, BST powdered ceramics are prepared using the conventional solid-state reaction [16, 17]. However, the synthesis of BST by solid-state reaction is time consuming, requires high temperature (above 1,100 °C) during synthesis. The synthesized powders normally have large particle size in the order of micrometers with a wide particle size distribution. Wet chemical routes, on the other hand, have been effective in lowering the synthesis temperature and reducing the particle size into nanometer range such as in precipitation techniques [18, 19], hydrothermal processes [20–23], solvothermal methods [24, 25] and sol–gel processes [26–29]. Nevertheless, the precipitation techniques [18, 19] require critical control of a large number of process variables such as pH that could complicate the synthesis process. In addition, phase impurity and stoichiometric deviation need to be taken into consideration. Hydrothermal [20–22] and solvothermal processes [23, 24] have the advantages of using much lower synthesis temperature (below 400 °C) and at low equipment cost. However, these methods tend to produce irregular-shaped nano particles with relatively wide size distribution, high degree of agglomeration, as well as significant phase impurity and stoichiometric deviation.

On the other hand, sol–gel processes [25–28] are commonly applied in the preparation of BST powders and thin films due to the precise control of composition, ease of homogenous distribution of elements, cost effective, and simple process requirements. However, the particle size, phase, and distribution control could be further improved. Most reported works in BST powder preparation by sol–gel process focused on injection of mixed precursor solutions by using pipette, syringe or programmable peristaltic pump. As the flow rate of the precursor solution could not be controlled exactly by syringe and pipette and in view of the relatively high cost of peristaltic pump, a simple dripping system with 21G (0.723 mm) diameter syringe was used in this study in order to provide slow injection of the Barium/Strontium precursor solutions into the mixed solutions of titanium iso-propoxide and ethylene glycol ethyl during the powder synthesis. This slow injection of precursor solutions offers improved rate-control of sol–gel synthesis and helps to assure good particle size control and phase homogeneity during the BST synthesis. The effects of the calcination temperature and the sintering temperature on the particle size control and also the dielectric performance of $Ba_{0.5}Sr_{0.5}TiO_3$ are then investigated. $Ba_{0.5}Sr_{0.5}TiO_3$ has been chosen due to superior electrical properties in the paraelectric phase as well as minimum aging and fatigue effects at room temperature [2]. In addition, reasonably high dielectric constant, low dielectric loss and low leakage current density [29] are possible. The higher content of Barium in $Ba_xSr_{1-x}TiO_3$ would lead to higher dielectric constant and charge storage density. At $x > 0.65$, the cubic structure eventually transformed into tetragonal phase which exhibits stronger ferroelectric nature, better tunability, and a nearly zero temperature coefficients [30, 31]. However, there are limited reports on the preparation and characterization of $Ba_{0.5}Sr_{0.5}TiO_3$ using sol–gel technique. In this paper, we investigated the new and relatively easy way of preparation of $Ba_{0.5}Sr_{0.5}TiO_3$ by slow injection sol–gel technique and its phase formation, surface morphology, and dielectric properties.

## Experimental

### Materials

Barium acetate (99%, Aldrich—24367), strontium acetate (99.995%, Aldrich—437883), and titanium (IV) iso-propoxide (97%, Aldrich—205273) were used as starting materials for the BST synthesis. Acetic acid was used as solvent, while the particles size and stability of the titanium iso-propoxide solution was controlled by adding ethylene glycol ethyl (99%, Aldrich—128082). All the acids and chemicals were of Analytical Reagent (A.R.) grade.

### Sample preparation

At the initial stage of $Ba_{0.5}Sr_{0.5}TiO_3$ synthesis, stoichiometric ratio of barium acetate, and strontium acetate were dissolved separately in acetic acid (Glacial 100%). The two precursor solutions were then mixed together to form 20 mL of barium strontium which was subsequently dripped into the solution containing titanium iso-propoxide and ethylene glycol ethyl using a syringe with diameter 0.723 mm (21G) at a flow rate of 2 mL/min. The resultant solution was constantly heated at 70 °C with continuous stirring at 240 rpm for 15 min over pH value in the range of 3.5–5. The slow-rate injection procedure enabled better control of the reaction to form the transparent gel.

The sol–gel process was accomplished in less than 30 min. The as-prepared BST gels were dried at room temperature for 24 h in air. The BST-dried gels were subsequently calcined at 600, 700, 750, 800, 900, 1000, and 1100 °C for 3 h, respectively, in a Carbolite muffle furnace and eventually ground into powder form by agate mortar and pestle.

## Thermal analysis and surface morphology

The thermal properties of the BST-dried gels were characterized using Thermal Gravimetric Analyzer (Mettler Toledo, TGA/SDTA851e) and Differential Thermal Analyzer (DTA, Perkin Elmer DTA 7) in the temperature range of 25 to 1,000 °C at the rate of 10 °C/min. The phase purity of the BST powders were examined by X-ray powder diffraction method (XRD, PW 3040) with CuK$\alpha$ radiation, $\lambda = 1.5406$ Å in the $2\theta$ range of 20° to 80°. The crystallite size was calculated according to Scherrer's formula.

Transmission Electron Microscopy (TEM) (Philips HMG 400) was deployed for the study of surface morphology and particle size of calcined barium strontium titanate powders. The calcined powders were initially sonicated for 10 min at 50 Hz. Subsequently, the samples were dropped onto 300 mesh Formvar grid and viewed under TEM. The average particle size of the samples was measured with the assistance of SIS (Soft Imaging System) iTEM software.

Nano particle size analyzer (Nanophox, Sympatec with software Windox 5.0) was employed for the study of particle size and the distribution of the calcined barium strontium titanate powders. The samples were dispersed in acetone as a dispersant prior to measurement. The particle size distribution [PSD] was analysed using dynamic light scattering (DLS) as a non-selective method to measure the cumulative size distribution and standard deviation. The results produced only one single peak for every multimodal technique.

## Dielectric characteristics

### *Sample preparation*

Pellets of $Ba_{0.5}Sr_{0.5}TiO_3$ calcined at 800, 900, 1000, and 1100 °C were prepared by a stainless steel die measuring 12 mm in diameter. Sufficient amount of powders were added, cold pressed uniaxially, and then sintered in order to increase the mechanical strength and to reduce the intergranular resistance in the pellets. The $Ba_{0.5}Sr_{0.5}TiO_3$ pellets, with an average thickness of 1.90 mm and a disc diameter of 12 mm, were then sintered in a heat-cool cycle at 1250, 1300, and 1350 °C, respectively, at a rate of 5 °C/min and a soaking time of 3 h. The entire process flow is summarized in Fig. 1.

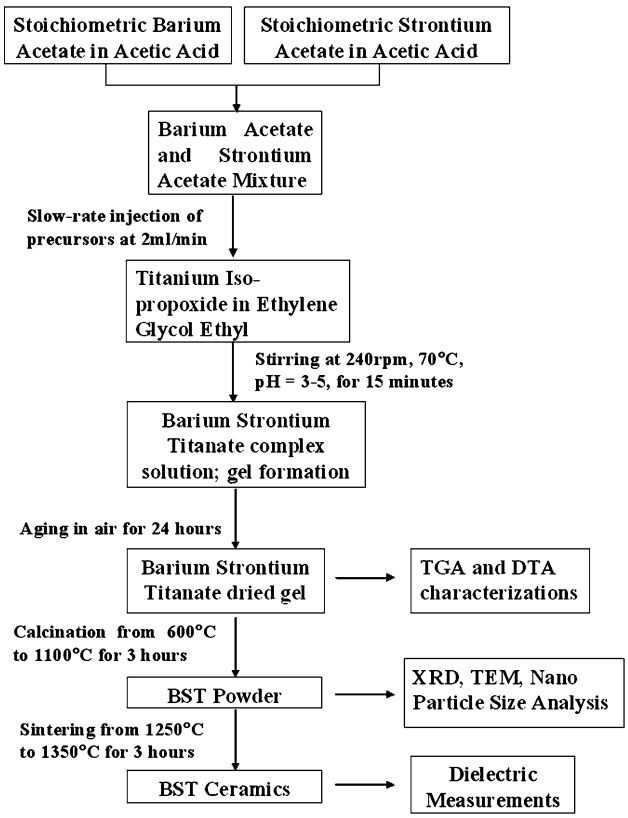


**Fig. 1** The flow chart illustrating the major process steps involved in the synthesis of $Ba_{0.5}Sr_{0.5}TiO_3$ nano powders and sintered ceramics

For capacitance measurements, both surfaces of the sintered $Ba_{0.5}Sr_{0.5}TiO_3$ pellets were polished by roll grinder (Buehler Handimet 2) and grinder polisher (Imptech 10 V). Electrodes were attached using silver pastes that were dried at 250 °C for 10 min. LCR meter (HP 4284A with test fixture 16451B) was employed to measure the capacitance ($C_p$) and dielectric loss ($D$) of the samples at ambient temperature. The LCR meter was calibrated for 1 V (rms) for $C_p - D$ measurements. The measurement frequency was varied from 100 Hz to 1 MHz and the corresponding $C_p - D$ data were recorded. The dielectric constants (corrected for geometric factor) were calculated by using the standard equation as given by $\varepsilon' = C_p/C_o$ where $\varepsilon'$ = dielectric constant and $C_o$ = the free space capacitance.

### *Leakage current characteristics*

The BST pellets were calcined at 800, 900, 1000, and 1100 °C, respectively, prior to final sintering at 1,350 °C. Samples attached with silver electrodes were tested for the leakage current using precision semiconductor parameter analyzer (Agilent 4156C). The leakage current measurements were conducted by varying the voltage from −10 to 10 V at temperatures 27 and 175 °C.

## Results and discussion

### DTA/TGA analysis

The DTA and TGA thermograms of the dried BST gels heated from 25 to 1,000 °C are shown in Fig. 2a and b, respectively. The first endothermic peak observed around 119 °C in DTA thermogram corresponds to 60% weight loss in TGA which may be attributed to the dehydration of solvents or moistures. The second endothermic peak observed around 341 °C and the exothermic peaks around 190, 273, and 453 °C in DTA thermogram which correspond to 20% weight loss in TGA could be due to the pyrolysis of residual organics. The weight loss stabilized once beyond 500 °C, indicating that most residual organics were removed. From these results, it is found that the initial formation of the $Ba_{0.5}Sr_{0.5}TiO_3$ phase took place above 500 °C [32], followed by crystallization. The relatively broad exothermic peaks feature around 610 and 710 °C could be due to the crystallization of various transient phases. As the calcining temperature was increased, the intensity of the transient phases weakened, and fully disappeared at the calcining temperature of 800 °C which is illustrated in Fig. 3.

### Crystalline structure

The phase formation of BST-dried gel was investigated at different calcination temperatures ranging from 600 to 1,100 °C. From the XRD patterns in Fig. 3, the samples calcined at temperatures below 800 °C have not been fully reacted. The reflection planes belonging to recalcitrant barium strontium carbonate (ICDD no: 47-223) at $2\theta$ of 24.48° and 34.9548°, respectively. In addition, extra peaks corresponding to $TiO_2$ is discernable at 27.41°. This clearly indicates that these calcination temperatures are not high enough to complete the desired chemical decomposition, and therefore, higher calcination temperatures are required for samples to reach thermo equilibrium [33]. Single phase $Ba_{0.5}Sr_{0.5}TiO_3$ was formed evidently at calcination temperature of 800 °C and above. This sample could be fully indexed based on cubic perovskite structure, and space group, Pm-3m, with $a = b = c = 3.9537$ Å and $\alpha = \beta = \gamma = 90°$, respectively. This agrees reasonably well with the ICDD number (00-039-1395). The BST samples prepared by solid-state method required minimum calcination temperature of 1,150 °C and firing duration between 2 and 5 h [16, 17]. However, co-precipitation method required minimum calcination temperature of 800 °C and a duration of 4 h [34]. The phase pure BST samples prepared in our work need only 800 °C for 3 h. The minimum calcination temperature for the formation of single phase BST nano powder is therefore lower than that of the solid-state reactions [16, 17] and completed in faster time duration than that of co-precipitation method. On the other hand, the dried gels calcined at higher temperatures (900, 1000, and

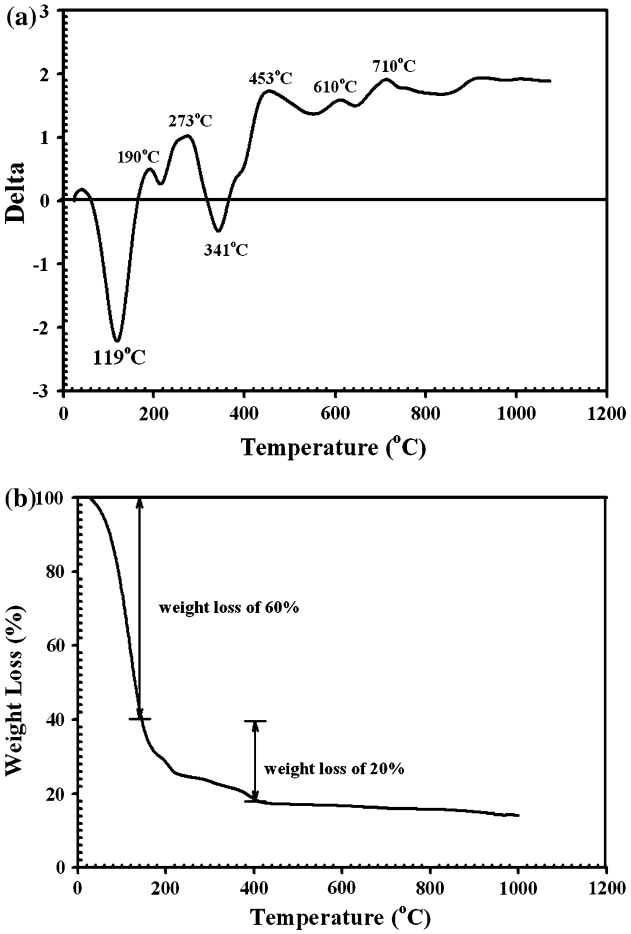


**Fig. 2** **a** DTA and **b** TGA for the BST-dried gels

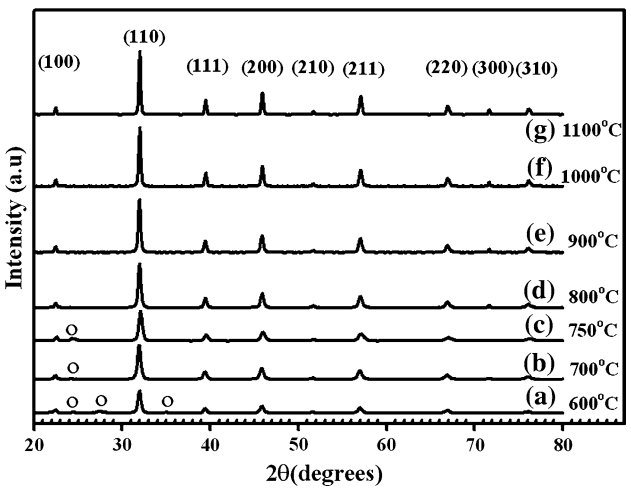


**Fig. 3** XRD patterns of BST powders calcined at (*a*) 600 °C, (*b*) 700 °C, (*c*) 750 °C, (*d*) 800 °C, (*e*) 900 °C, (*f*) 1000 °C, and (*g*) 1100 °C. (*open circle* indicates position of intermediate phases of titanium oxide and barium strontium carbonate detected)

**Table 1** The crystallite sizes from Scherrer formula based on XRD analysis, the particle sizes from TEM/particle size analyser for $Ba_{0.5}Sr_{0.5}Tio_3$ nano crystals calcined from 800 to 1,100 °C, respectively

| Calcination temperature (°C) | Crystallite size by XRD (nm) | Average particle size by TEM (nm) | Particle size analyzer | |
|---|---|---|---|---|
| | | | Average size (nm) | Standard deviation (nm) |
| 800 | 36 | 42 | 43 | 3.48 |
| 900 | 37 | 56 | 76 | 4.13 |
| 1,000 | 42 | 77 | 93 | 7.09 |
| 1,100 | 51 | 145 | 166 | 16.60 |

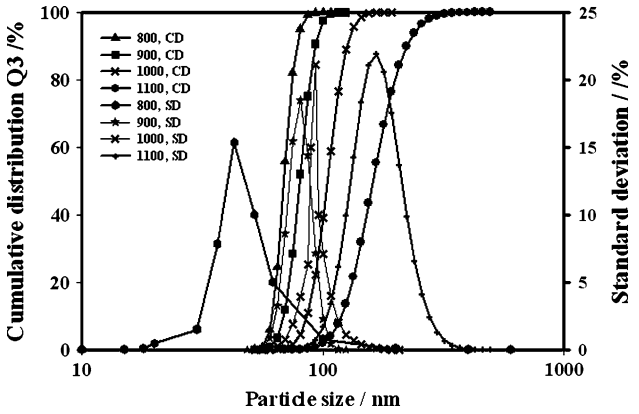


**Fig. 4** Cumulative distribution and standard deviation of BST calcined at different temperatures

1100 °C) show higher intensities in their reflection planes, indicating better crystallinity in the structure. The crystallite sizes of the $Ba_{0.5}Sr_{0.5}TiO_3$ nano crystals formed at different calcination temperatures were calculated using Scherrer's formula as listed in Table 1. It is observed that crystallite size increases with the calcination temperature. The sample which was calcined at 800 °C exhibits the smallest crystallite size of 36 nm.

## Particle size analysis

The size of the $Ba_{0.5}Sr_{0.5}TiO_3$ nano particles as measured by the nano particle size analyzer are summarized in Table 1. $Ba_{0.5}Sr_{0.5}TiO_3$ sample calcined at 800 °C has the smallest particle size with an average particle size of 42 nm which is in good agreement with that calculated using Scherrer's formula. The standard deviation of the particle size is only ±4 nm, indicating clearly that the particles in the $Ba_{0.5}Sr_{0.5}TiO_3$ sample are highly uniform with a narrow particle size distribution. However, there is an increasing trend in average particle size and the standard deviation when the calcination temperature increased,

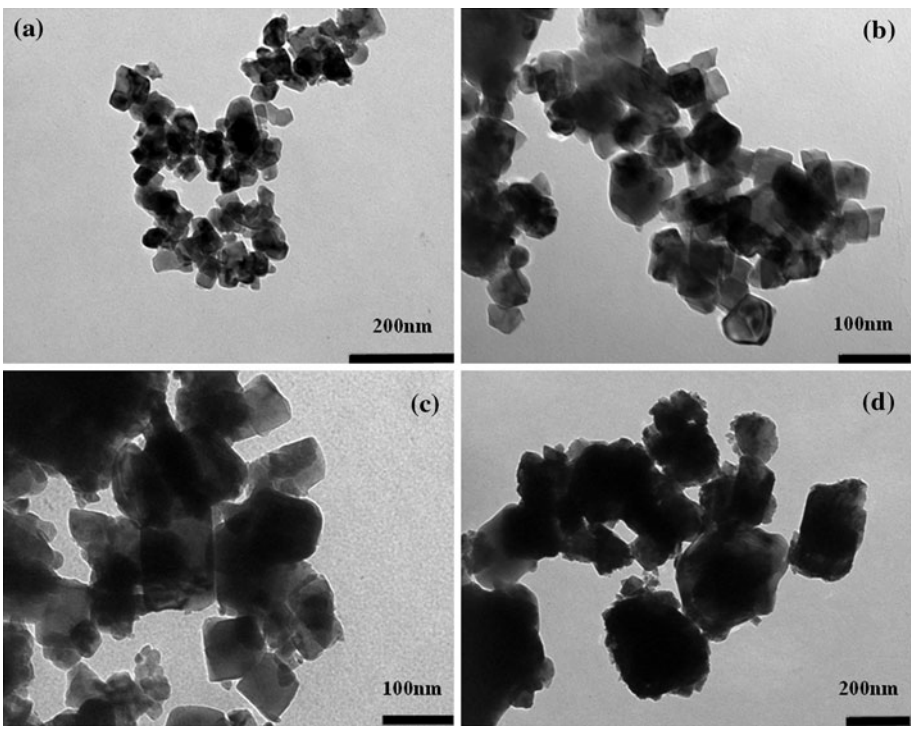


**Fig. 5** TEM images of $Ba_{0.5}Sr_{0.5}TiO_3$ calcined at **a** 800 °C, **b** 900 °C, **c** 1000 °C, and **d** 1100 °C

above 800 °C, as shown in Fig. 4. The increment of particle size at higher temperature is probably due to the agglomeration as evidently shown in TEM images (Fig. 5a–d).

Table 1 showed the $Ba_{0.5}Sr_{0.5}TiO_3$ crystallite size and particle size measured by different methods. Particle size is referred to the diameter of a grain and crystallite size is the size of a single crystal inside the grain, therefore, it is expected that crystallite size is smaller than the particle size. Both TEM and Particle Size Analyzer were used to measure particle size. TEM was used to identify the shape as well as the diameter of the specific individual particles; as for Particle Size Analyzer, the measurement is based on laser diffraction method to determine the distribution of particle size from large amount of particles randomly. Based on Table 1, as the calcination temperature increased, both crystallite size and particle size increased; this is due to the grain growth as calcination temperature increased. The standard deviation value calculated from the particle size distribution by Particle size analyzer indicated that the synthesized powder has good uniformity with a narrow particle size distribution.

The TEM images of the calcined $Ba_{0.5}Sr_{0.5}TiO_3$ samples from 800 to 1,100 °C are shown in Fig. 5a–d. In general, $Ba_{0.5}Sr_{0.5}TiO_3$ particles are of cubic shape and with certain degree of agglomeration; the particles are larger as the calcination temperature increased (from Fig. 5a to d). The average particle size of the samples was measured with the help of SIS (Soft Imaging System) iTEM software attached with the TEM, Philips HMG 400) system. In addition, highly homogenous nano particles with an average particle size of 42 nm and the smallest particle size of 36 nm were observed for the $Ba_{0.5}Sr_{0.5}TiO_3$ nano particles calcined at 800 °C. As listed in Table 1, the TEM data complement well with both results obtained by XRD and particle size analyzer. In addition, it is shown that the particle size of the $Ba_{0.5}Sr_{0.5}TiO_3$ nano particles increases with the calcination temperature. At temperature above 1,000 °C, the particles experienced grain growth process and subsequently formed larger particles due to higher temperature during calcination process.

## Dielectric constant and dielectric loss

Figure 6a, b shows the variation in the dielectric constant and the dielectric loss measured at a frequency of 1 kHz for $Ba_{0.5}Sr_{0.5}TiO_3$ pellets calcined from 800 to 1,100 °C, and sintered from 1,250 to 1,350 °C, respectively. Similar trends are observed for frequencies from 100 Hz to 1 MHz from the capacitance measurements. There is an obvious correlation between the decrease in dielectric constant and the increase in dielectric loss with the increase in the particle size of the sintered samples, when the calcination temperature was increased under similar sintering

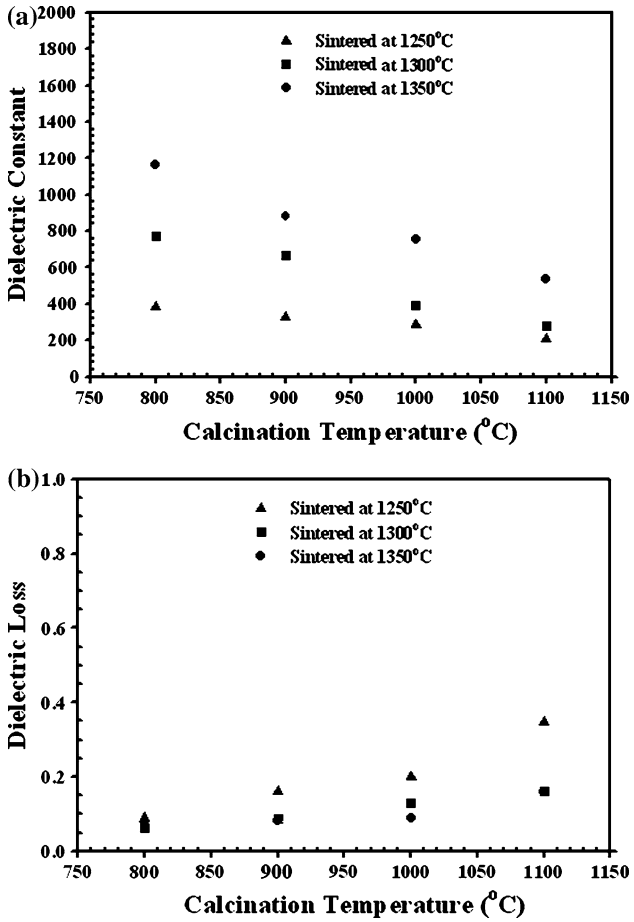


**Fig. 6** The room temperature variation of **a** dielectric constant, and **b** dielectric loss as a function of calcination temperature and sintering temperature for $Ba_{0.5}Sr_{0.5}TiO_3$ samples, measured at 1 kHz, respectively

conditions. On the other hand, the dielectric constant increased and the dielectric loss decreased when the sintering temperature was increased at similar calcination conditions. Higher sintering temperature usually contributes to denser sample and thus, the observed dielectric performance. As a result, relatively higher dielectric constant and lower dielectric loss are obtained for $Ba_{0.5}Sr_{0.5}TiO_3$ samples calcined at 800 °C and higher sintering temperatures. The highest values recorded within the investigated range for dielectric constant and dielectric loss measured at 1 kHz are 1,164 and 0.063, respectively, for the $Ba_{0.5}Sr_{0.5}TiO_3$ pellets calcined at 800 °C and sintered at 1,350 °C.

## Leakage current measurements

Figure 7a–d shows the I–V characteristics of BST pellets coated with silver as electrodes, calcined at 800, 900, 1000, 1100, and sintered at 1350 °C, respectively. Measurements were made at the temperatures of 27 °C (300 K) and

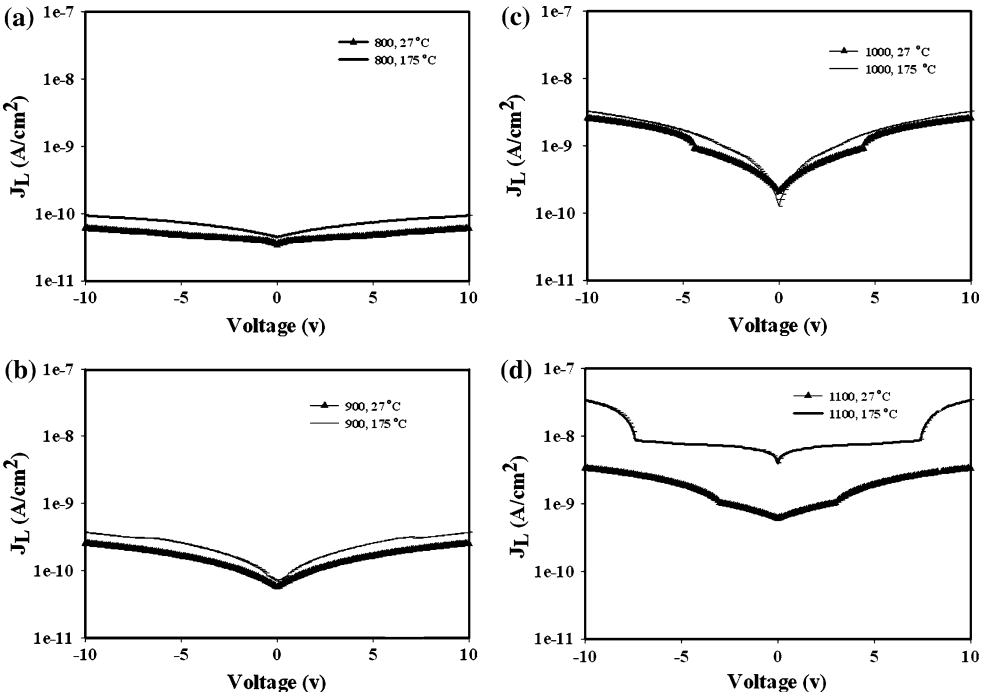


**Fig. 7** I–V characteristics of $Ba_{0.5}Sr_{0.5}TiO_3$ calcined at **a** 800 °C, **b** 900 °C, **c** 1000 °C, and **d** 1100 °C, sintered at 1350 °C, and measured at 27 and 175 °C, respectively

175 °C (448 K), respectively, in order to identify the dominant leakage mechanism in the BST samples. The symmetry of the curves indicate the same barrier height for both silver top and bottom electrodes due to the similar work function [35]. In Fig. 7a, when the calcination temperature was 800 °C and at measuring temperatures of 27 and 175 °C, the slopes are not obvious, meaning that the resistance in BST oxide material is high and hence lower leakage current density. However, when the calcination temperature was increased to 900 and 1,000 °C, two distinctive slopes in the 0–5 V and 5–10 V regions, respectively, are observed. But, when the calcination temperature was increased to 1,100 °C at the measuring temperature of 175 °C, the low voltage region is extended to 0–7.4 V. The leakage mechanism of BST is usually described by Ohmic conduction in the low voltage region, and by Poole–Frankel emission or Schottky emission in the high voltage region [6]. It is clear from the results that the BST calcined at 1,100 °C, which contains a large average grain size of 145 nm, exhibits a much higher leakage current density of 7.72 and 1.93 μA/cm$^2$ measured at 175 °C and room temperature, respectively. In contrast, BST calcined at the calcination temperature of 800 °C, with an average grain size of 42 nm, shows the lowest leakage current density of 73.5 nA/cm$^2$ measured at 175 °C, and 49.4 pA/cm$^2$ at room temperature which are below the typically required leakage threshold. In general, the leakage properties of BST samples depend on a variety of factors such as microstructure, stoichiometry, electrode materials, sintering treatments, charge density, and distribution [36]. The variation in leakage currents may include slight changes in microstructure or composition caused by slight variations of the processing parameters, as leakage will be very sensitive to the defect microstructure [37]. The results shown here are likely attributed to the grain boundary effect, i.e., large grains developed in the BST at higher calcination temperature. However, lower calcination temperature could result in smaller grain size, and therefore, large number of grain boundaries. These grain boundaries are highly resistive in nature, which inhibits charge-transfer across the material [38, 39]. At a constant applied voltage (5 V), larger number of grain boundaries leads to decrease in the voltage per grain boundary and hence decrease of the leakage current. Even at the measuring temperature of 175 °C, the leakage current changes according to the calcination temperature, which effectively determine the grain morphology of the BST. On the other hand, this is also likely due to a wider energy band-gap in which samples with smaller grain size exhibit larger band-gap energies and longer leakage pathway if compared to samples with larger grains [40]. Hence, it has been concluded that the leakage currents are found to increase with preliminary calcination temperature for the same sample. This result suggests that the electrical properties of the BST can be tailored by controlling the calcination temperature, resulting in the different grain size in the BST films. Further work in vaporising BST on Ni–Fe thin films on copper substrates for BST thin film based capacitors are in progress.

## Conclusions

Highly uniform nanoparticles of $Ba_{0.5}Sr_{0.5}TiO_3$ were successfully synthesized using a simple slow precursor injection procedure in standard sol–gel process. Single phase cubic perovskite structure of $Ba_{0.5}Sr_{0.5}TiO_3$ was achieved at a calcination temperature of 800 °C. The $Ba_{0.5}Sr_{0.5}TiO_3$ nano powder synthesized is highly homogenous with a narrow size distribution. At room temperature, optimum dielectric constant and dielectric loss can be achieved in sintered $Ba_{0.5}Sr_{0.5}TiO_3$ ceramics calcined at 800 °C and sintered at 1,350 °C, with the lowest particle size and the lowest leakage current density for a $Ba_{0.5}Sr_{0.5}TiO_3$ pellet capacitor.

**Acknowledgements** The authors are grateful to the Ministry of Science, Technology and Innovation (MOSTI), Malaysia for supporting this study under eScience Fund (Project No. 03-02-01-SF0059) as well as Ms Zaidina Bt Mohd Daud, Mr Sharul Ami b. Zainal Abidin and Mr Kenny Gan Chye Siong for their assistance with the characterizations.

## References

1. Tahan DM, Safari A, Klein LC (1996) J Am Ceram Soc 79:1593
2. Parker LH, Tasch AF (1990) IEEE Circuits Devices Mag 6:17
3. Ming-Chieh C, Chun-Feng C, Wen-Tang W, Fuh-Sheng S (2005) J Electrochem Soc 152:F66
4. Zhang R-B, Yang C-S, Ding G-P (2005) Mater Lett 59:1741
5. Auciello O, Saha S, Kaufman DY, Streiffer SK, Fan W, Kabius B, Im J, Baumann P (2004) J Electroceram 12:119
6. Miao J, Chen W-R, Chen B, Yang H, Peng W, Zhong J-P, Wu H, Yuan J, Xu B, Qiu X-G, Cao L-X, Zhao B-R (2004) Chin Phys Lett 21:1139
7. Zhu X, Zheng D, Peng W, Miao J, Li J (2004) J Cryst Growth 268:192
8. Hochul K, Sungho P, Kyekyoon K, Man YS, Hyungsoo C (2004) Electrochem Solid-State Lett 7:F77
9. Chiu MC, Wang CC, Yao HC, Shieu FS (2005) Mater Chem Phys 94:141
10. Xia Y, Wu D, Liu Z (2004) J Phys D 37:2256
11. Morito K, Suzuki T, Kishi H, Sakaguchi I, Ohashi N, Haneda H (2007) IEEE Trans Ultrason Ferroelectr Freq Control 54:2567
12. Roy SC, Sharma GL, Bhatnagar MC, Manchanda R, Balakrishnan VR, Samanta SB (2004) Appl Surf Sci 236:306
13. Lee JM, Kang SY, Shin JC, Kim WJ, Hwang CS, Kim HJ (1999) Appl Phys Lett 74:3489
14. Cheol Seong H, Byoung Taek L, Chang Seok K, Jin Won K, Ki Hoon L, Hag-Ju C, Hideki H, Wan Don K, Sang In L, Young Bum R, Moon Yong L (1998) J Appl Phys 83:3703
15. Yang X, Yao X, Zhang L (2004) Ceram Int 30:1525
16. Su B, Holmes JE, Cheng BL, Button TW (2002) J Electroceram 9:111
17. Berbecaru C, Alexandru HV, Porosnicu C, Velea A, Ioachim A, Nedelcu L, Toacsan M (2008) Thin Solid Films 516:8210
18. Fang T-T, Lin H-B, Hwang J-B (1990) J Am Ceram Soc 73:3363
19. Packia Selvam I, Kumar V (2002) Mater Lett 56:1089
20. Bonnie MMLRER, Gersten L (2004) J Am Ceram Soc 87:2025
21. Reveron H, Elissalde C, Aymonier C, Bousquet C, Maglione M, Cansell F (2006) Nanotechnology 17:3527
22. Xu H, Karadibhave S, Slamovich EB (2007) J Am Ceram Soc 90:2352
23. Wei X, Xu G, Ren Z, Wang Y, Shen G, Han G (2008) J Cryst Growth 310:4132
24. Hou B, Xu Y, Wu D, Sun Y (2006) Powder Technol 170:26
25. Nazeri A, Kahn M, Kidd T (1995) Mater Sci Lett 14:1085
26. Lahiry S, Gupta V, Sreenivas K, Mansingh A (2000) IEEE Trans Ultrason Ferroelectr Freq Control 47:854
27. Majumder SB, Jain M, Martinez A, Katiyar RS, Keuls FWV, Miranda FA (2001) J Appl Phys 90:896
28. Somani V, Kalita S (2007) J Electroceram 18:57
29. Jia QX, Wu XD, Foltyn SR, Tiwari P (1995) Appl Phys Lett 66:2197
30. Fu C, Yang C, Chen H, Wang Y, Hu L (2005) Mater Sci Eng B 119:185
31. Reisinger H, Stengl R (2000) In: Proceedings of the 2000 third IEEE international Caracas conference D26/1
32. Shen C, Liu Q-F, Liu Q (2004) Mater Lett 58:2302
33. Lu Q, Chen D, Jiao X (2003) J Alloys Compd 358:76
34. Li M-l, Liang H, Xu M-X (2008) Mater Chem Phys 112:337
35. Wang YK, Tseng TY, Lin P (2002) Appl Phys Lett 80:3790
36. Li J et al (2005) Model Simul Mater Sci Eng 13:699
37. Dietz GW, Schumacher M, Waser R, Streiffer SK, Basceri C, Kingon AI (1997) J Appl Phys 82:2359
38. Tsai MS, Tseng TY (1999) J Phys D 32:2141
39. Vollmann M, Hagenbeck R, Waser R (1997) J Am Ceram Soc 80:2301
40. Tian H-Y, Choi J, No K, Luo W-G, Ding A-L (2003) Mater Chem Phys 78:138